TECHNISCHE MECHANIK, Band 23, Heft 1, (2003), 1-9
Manuskripteingang: 30. Mai 2002

An Investigation of the Chip Segmentation Process Using Finite Elements

M. Bäker

A finite element model of a two-dimensional orthogonal metal cutting process is used to simulate the formation of segmented chips. The deformation of the chip during segmentation is studied and the distribution of deformation energy in chip and shear band is analyzed. It is shown that the plastic deformation both in the shear band and the segment contribute significantly to the cutting force. A variation of the thermal conductivity strongly affects the segmentation and indicates that segmentation is energetically favorable.

1 Introduction

Machining is a process of great industrial importance, as many complex-shaped components can only be formed by cutting or milling. To understand the physics underlying metal cutting operations may help to improve the technique and thus lead to enormous cost savings, but is also interesting because of the high complexity of the chip formation process. Figure 1 shows a micrograph taken from a quickstop-experiment, where a cutting operation is abruptly halted and the chip is "frozen". The chip in this case is not homogeneously deformed, but has a strongly serrated shape. Regions of high plastic deformations (shear bands) interchange with regions where the deformation is rather small. Such segmented chips are often formed, especially at high cutting speeds.

The shear localization that is apparent in the segmented chip can only occur in the presence of a softening mechanism, making deformation of an already deformed region easier than that of an undeformed region (see Recht, 1985 or Hou and Komanduri, 1997). As segmented chips usually form at high cutting speeds, this softening is often due to the rise in temperature caused by energy dissipation.

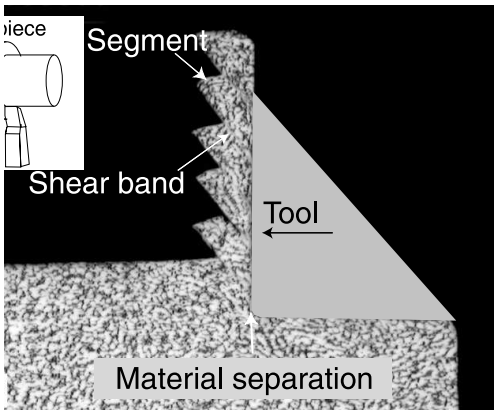

Figure 1: Quickstop-picture of a chip formation process for Ti6Al4V for a cutting speed of 20 m/s, cutting depth of 126 µm and rake angle 0°. The formed chip is strongly segmented, i.e. strongly deformed regions (shear bands) change with more weakly deformed ones. The inlay schematically shows a turning process.

An alternative mechanism for chip segmentation has also been proposed where the segmentation is not caused by shear localization, but rather by cracks growing in the material (Nakayama, 1974; Vyas and Shaw, 1999). Finite element simulations of this process have also been performed in the past (Obikawa and Usui, 1996; Bäker et al., 2002a). Here we assume that such cracks do not play a role in the segmentation process.

In this paper a finite element simulation of the chip formation process is used to study the different stages of the segmentation process. After a brief discussion of the finite element model, the question of choosing an appropriate material law is considered. At the moment, the material behaviour at the strains and strain rates involved in high-speed cutting is hardly understood. For the purpose of this paper, a simple isotropic plastic flow law is assumed. The formation of a chip segment is studied in some detail and the amount of energy dissipated in the different regions of the chip is evaluated. Finally, a variation of the thermal conductivity of the material is performed.

2 The Model

2.1 Finite Element Model

A two-dimensional plane-strain fully coupled thermo-mechanical implicit finite element model of the machining process with orthogonal cutting conditions is used in this work. First-oder quadrilateral elements with selectively reduced integration were chosen throughout the model. As strong deformations are to be expected when a shear band forms, it is mandatory to use a frequent remeshing process in order to ensure that distortions of the elements do not become too severe. The simulation was therefore interrupted in regular intervals or whenever serious convergence problems arose and a new mesh was calculated conforming to the actual boundaries of the material. The finite element software ABAQUS/Standard (HKS Inc., 1998a) used allows the automatic interpolation of all solution and state variables from the old to the new mesh. Depending on the shape of the chip, the number of elements was between 5000 and 15000. A detailed description of the model can be found in Bäker et al. (2002b).

Figure 2 shows a detail of the element mesh after a remeshing step. The topology of the mesh is well-adapted to that of the chip and reentrant corners on the back side do not cause distortions in the element shapes. The mesh is refined in the primary shear zone by putting an additional node onto the edge of an element on the side where mesh refinement is desired and thus doubling the number of elements (see Figure 2). The degrees of freedom of the node on the midside of the element edge are fixed by linear interpolation of the adjacent nodes. This method allows refinement without the use of trapezoidal elements, thus avoiding strongly acute element angles, and is described in more detail in HKS (1998a).

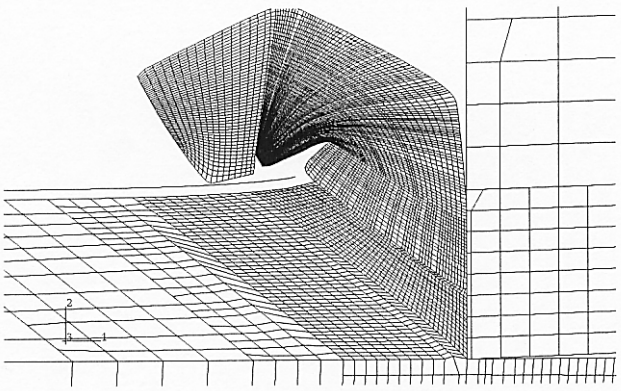

Figure 2: Finite element mesh of the segmented chip. Note the strong refinement in the shear zone. Frequent remeshing ensures that mesh distortions are small. Seemingly "free" nodes are fixed using a constraint equation.

The tool has been assumed to be perfectly rigid and frictionless and no heat conduction into it was possible. This simplification was used so that all heat in the model is generated by plastic deformation. As the thermal conductivity of the titanium alloy under consideration is low, heat generated on the rake face will not strongly influence the conditions in the shear band.

One of the main problems of simulating a machining process is the correct representation of material separation in front of the tool tip. Different techniques have been advocated in the past, see e.g. Huang and Black (1996) and Sekhon and Chenot (1993). In this model, the material is assumed to flow around the tool tip, i.e. no separation of nodes is necessary. This has the advantage that the line of separation need not be fixed beforehand. However, when the tool advances, it will cut through one element so that one node of the element lies on the rake and the other on the flank face, resulting in some overlap of

the workpiece material with the tool. This overlapping material is removed during the next remeshing step and corresponds to a small strip of roughly 1 µm thickness in a simulation with a cutting depth of 35 µm. This overlap leads to an artificial increase in the cutting force as the overlapping material has to be strained by the tool. Some simulations have also been performed using a node separation technique, where material separation occurs along a predefined node separation line, when the nodes reach a critical distance from the tool tip. As material separation in this case occurs in front of the tool tip, the cutting force is underestimated. The calculated cutting forces for the node separation model were about 10% smaller in this case, showing that the influence of the separation technique is not too large. Furthermore, the deformation pattern of the chip did not differ significantly between the two models. For further details, the reader is again referred to Bäker et al. (2002b).

2.2 Material Law

During high-speed metal cutting material deforms with extremely high plastic deformation rates. For the case of Titanium alloys discussed here the deformation rate is of the order of $10^7\,\mathrm{s}^{-1}$ for a cutting speed of 20 m/s. High-speed deformation experiments, using, e.g., a split-Hopkinson-bar apparatus, can only reach strain rates of the order of $10^4\,\mathrm{s}^{-1}$ and thus have to be extrapolated over several orders of magnitude. Furthermore, the total equivalent strain in the shear zone may reach values of 1000%. Split-Hopkinson-bar experiments, on the other hand, yield only reasonable results when the specimen is homogeneously deformed, which, in the case of the alloy Ti6Al4V, means an equivalent plastic strain smaller than 20%. Thus it is not possible to get material data in parameter regions where shear localization occurs. This difficulty poses a severe problem for any finite element simulation of high-speed-cutting processes. Until the material behaviour during shear localization at high strain rates is better understood, no finite element simulation can be expected to yield quantitatively accurate results in the high-speed cutting regime.

Nevertheless, finite element simulations can give valuable insights into the details of the segmentation process, even if a simplified material law is assumed. It will be shown below that the greatest part of the cutting force is needed before shear localization begins, and that after localization starts, the segment itself is not strongly deformed anymore. This means that the onset of the localization process and the deformation inside the chip segments is not strongly influenced by the material behaviour during adiabatic shearing. The strength of the segmentation, however, which is determined by the deformation within the shear band, probably cannot be predicted reliably with such a model, and only comparisons with experiments can show whether the overall deformation pattern is realistic or not.

For this study we assume that the plastic behaviour can be described by a simple isotropic v. Mises flow stress law (see HKS (1998b) for details on the mathematical formulation and the numerical implementation of this law into the used finite element software). Similar approaches were used by Marusich and Ortiz (1995), Ng and Aspinwall (2000) and other groups. We use a material law for the alloy Ti6Al4V determined by El-Magd and Treppmann (2001) in a modified form. The isothermal flow stress σ of the material is given by

$$\sigma(\epsilon, \dot{\epsilon}, T) = K(T) \cdot \epsilon^{n(T)} \cdot (1 + C \ln(\dot{\epsilon}/\dot{\epsilon_0})) \tag{1}$$

where ϵ is the total equivalent plastic strain, $\dot{\epsilon}$ is the strain rate, K and n are temperature-dependent material parameters, and C and $\dot{\epsilon_0}$ are constant.

The temperature dependence of the parameters has the form

$$K(T) = K^* \Psi(T) \tag{2}$$

$$n(T) = n^* \Psi(T) \tag{3}$$

$$\Psi(T) = \exp\left(-\left(\frac{T}{T_{MT}}\right)^{\mu}\right) \tag{4}$$

K^*, n^*, T_{MT} and μ are fitted from the experiments. This means that the flow stress is extrapolated over four orders of magnitude in the strain rate and over nearly two orders of magnitude in the strain. Thus it is implicitly assumed that even during adiabatic shearing the plastic deformation can be described by eq. (1). Material parameters are given in Table 1.

The material law proposed by El-Magd and Treppmann (2001) uses a linear instead of a logarithmic strain rate dependence. In this case the yield strength at high strain rates has extremely large values

Mechanical	C	$\dot{\epsilon_0}$ [s^{-1}]	K^* [MPa]	n^*	T_{MT} [K]	μ
data	0.302	774	2260	0.339	825	2

Thermophysical	Thermal cond. [J/sKm]		Specific heat [J/kgK]		Expansion coefficient [10^{-6}]	
data	at 24 °C	at 1185 °C	at 24 °C	at 1185 °C	at 100 °C	at 1200 °C
	6.785	24.357	502	756	10.064	12.42

Table 1: Material Data Used in the Simulations.

of the order of magnitude of the Young's modulus of the material, leading to extremely high cutting forces and to purely elastic deformations of more than 10%. As this is not realistic, a logarithmic rate dependence was assumed here, fitting the constants C and $\dot{\epsilon}$ so that the flow stress of eq. (1) agrees with that given by El-Magd and Treppmann (2001) at strain rates of $10^3\,s^{-1}$ and $10^4\,s^{-1}$ for a temperature of 673 K and a strain of 10%. The resulting fit of the experimental data suffers from this procedure with deviations between measured values and those predicted by eq. (1) of up to 30% at high temperatures. Furthermore, as it is expected theoretically that the strain rate dependence should be linear at high strain rates, this procedure is not completely satisfactory.

Another parameter which is of importance for shear localization is the amount of mechanical work dissipated into heat, as this strongly influences the temperature of the material and thus the thermal softening. Again, reliable measurements of this parameter are not available, so that it was simply set to a value of 0.9.

For the reasons discussed before, it is clear that the material law does not describe the plastic flow behaviour of Ti6Al4V accurately in the parameter regions valid for metal cutting. The material used in the simulation should rather be considered as a model material with a simple plastic flow behaviour that leads to the formation of segmented chips as shown in the following section.

3 Results

3.1 The Process of Segmentation

Figure 3 shows the equivalent plastic deformation for different stages of the segmentation process for the simulation of high-speed cutting of the material discussed in Section 2.2 using a cutting speed of 20 m/s, a cutting depth of 35 µm and a rake angle of 0°. The third segment in the chip was chosen for a detailed study, as quickstop-experiments and simulations show that this segment is typical and exhibits no more influence from the startup of the process.

The chip formation process begins with the damming of material in front of the tool. The positions of nine points in the chip material during the cutting process are shown in the figure. It is apparent how the shear band formation separates points that lie closely together at the beginning of the process. The shear band starts at the tool tip and extends in a nearly straight line to the back of the workpiece. This is interesting, as some heuristic models of the chip formation process (e.g. Recht, 1985) assume a strongly curved shear band at the beginning of the shear localization process, although others (Hou and Komanduri, 1996) assume a straight shear band. The plastic deformation strongly concentrates inside the shear band, leading to the separation of points that were initially very close. The shear band then splits in front of the tool, causing deformation of a larger region of material. This has been discussed in more detail in Bäker et al. (2002b). The chip segments do not show a homogeneous deformation pattern. The deformation on the segment's back side is rather small, whereas the lower part of the segment is heavily deformed.

The calculated cutting force is shown in Figure 3(f). During the damming of the material the cutting force increases, dropping sharply when the shear band begins to form. The average cutting force has a value of 84 N, to be compared with an experimental value of 70 N, as measured by Hoffmeister et al. (1999). Considering the uncertainties in the material law, the agreement is reasonable. Time-resolved measurements show, however, that the cutting force in the experiment may break down by a factor of 4 or 5, which is much larger than in the simulation (U. Schreppel, private communication).

The degree of segmentation is smaller in the simulation than in the experiment (see Figure 1). This is probably caused by the fact that Titanium alloys show isothermal softening at larger strains, a phe-

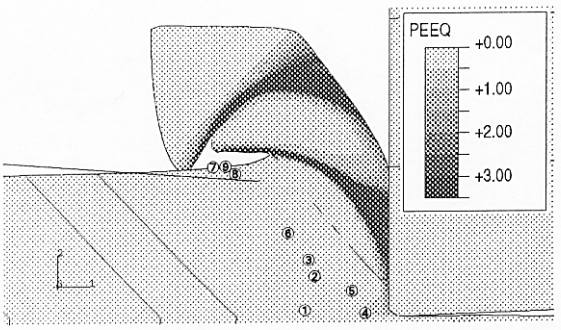

(a) 2.5µs

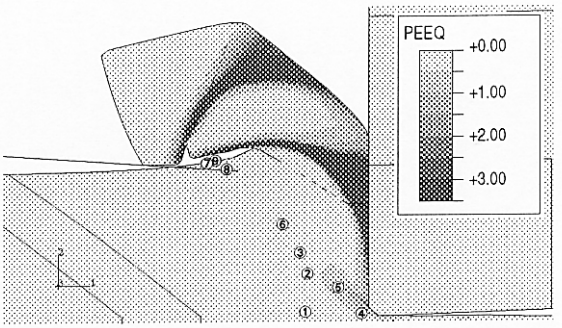

(b) 2.75µs

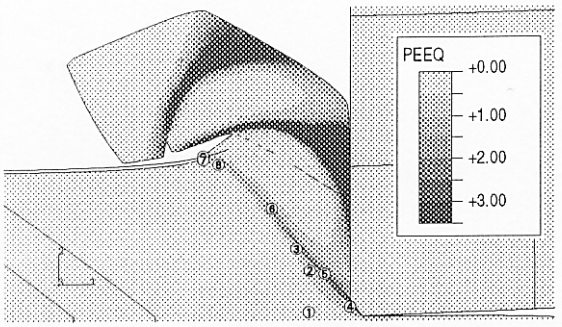

(c) 3µs

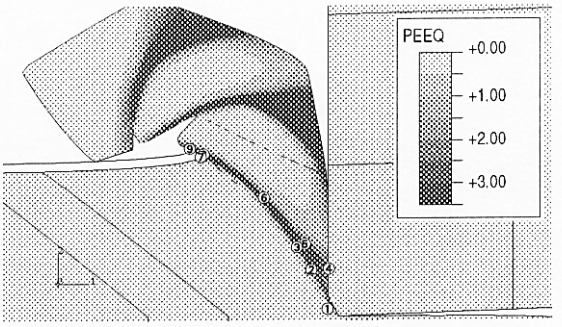

(d) 3.25µs

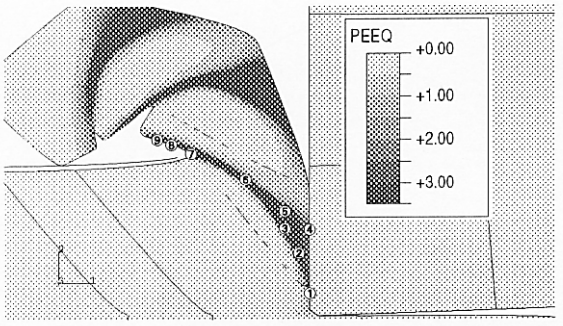

(e) 3.5µs

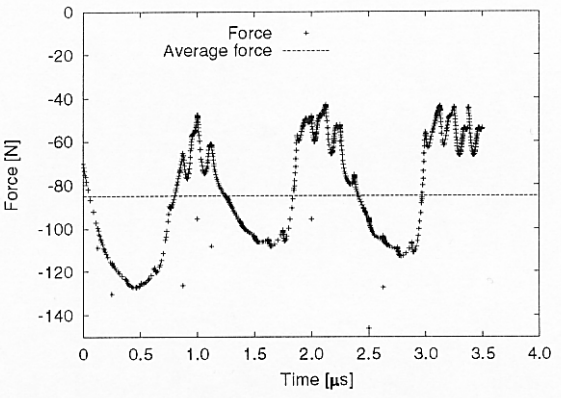

(f) Cutting force

Figure 3: (a)-(e): Contour plot of the equivalent plastic strain at different stages of the segmentation process. As the strains may become very large inside the shear band, the darkest colour in the scale corresponds to all values larger than 3. The numbered points shown are markes fixed to different material points. (f) shows the calculated cutting force over time for the same simulation and the average cutting force. Model parameters: cutting depth 35 µm, cutting speed 20 m/s, rake angle 0°.

nomenon not covered by equation (1), and by the unknown material properties during adiabatic shearing, see Section 2.2. A further discrepancy is observed in the chip curvature, which is much stronger in the simulation than in the experiment.

The discrepancies between simulation and experiment confirm that the material behaviour during adiabatic shearing is not correctly represented in the model. The global cutting force is not strongly influenced by this, as will be shown below, but its time-dependence and the degree of segmentation are. This again stresses the model character of the material law used for this study.

3.2 Energy Distribution

As dynamic forces and friction are neglected in this study, the total work done by the tool is used to deform the workpiece material. As the elastic strains are small, the work needed to elastically deform the material is neglected in the following considerations. Thus, all the stress-work is turned into dissipated energy during the deformation.

The distribution of the total dissipated energy in shear band and segment is of special interest, not only for a better understanding of the cutting process itself, but also with regard to a possible process optimization. To analyze this distribution, the amount of deformation work dissipated in regions with a certain equivalent plastic deformation was evaluated. Figure 4(a) shows the total energy dissipated by plastic deformation in the upper half of the material (above the separation line, called chip), the lower half of the material (called workpiece) and the energy dissipated in regions with a plastic deformation above and below two different threshold values in the chip. Thus it can be seen that the greatest part of the energy of the chip is dissipated in the region with an equivalent plastic deformation larger than 1.15 ($\times$)[1]. Thus more energy is dissipated in the strongly sheared regions than in the segments, despite the fact that the segment itself has a larger volume. Nevertheless, it can be seen that the energy dissipated in the segment (below a threshold value of 1.15, $\square$) is approximately 40% of the total dissipated energy and can therefore not be neglected.

A closer look at the curves for $\epsilon < 1.15$ and $\epsilon < 3$ shows that the energy dissipated in these regions diminishes when shear localization begins. This seemingly unphysical phenomenon is due to the fact that on exceeding the threshold value elements do not belong to these groups anymore, so that energy is "lost" from these groups. The fact that about 60% of the energy is dissipated in the regions with $\epsilon > 1.15$ therefore does not mean that this energy has been dissipated after the threshold value was reached, but only that it was dissipated in elements that eventually have a deformation larger than 1.15.

This has been accounted for in Figures 4(b) and 4(c). In Figure 4(b) only that part of the energy that has been dissipated after the threshold value was reached is plotted. This energy value is considerably smaller, showing that the dissipation of energy in the shear band is reduced with increasing deformation. This is of course caused by the increase in the temperature and the subsequent thermal softening, and it is accompanied by the strong drop in the cutting force shown in Figure 3(f). Figure 4(c) shows the energy that has been dissipated before the threshold value of the plastic deformation has been reached, and is thus the complement to Figure 4(b). More than half of the energy is dissipated before the plastic deformation exceeds a value of 1.15.

The value of the cutting force is thus mainly determined by the plastic deformation in the beginning of the shear band and in the lower part of the chip. After the chip has formed, the dissipation by plastic deformation is strongly reduced. It can also be seen from the figure that after the shear localization starts, the energy in the non-sheared regions does not increase anymore, showing that nearly no plastic deformation occurs in the already formed segment.

From these considerations it can be concluded that any heuristic model of the segmentation process must neither neglect the work done in the shear bands nor that dissipated inside the rather weakly deformed regions in the segment.

[1] 1.15 was chosen as a threshold value as this is the minimum value of plastic deformation in a continuous chip (Merchant, 1945).

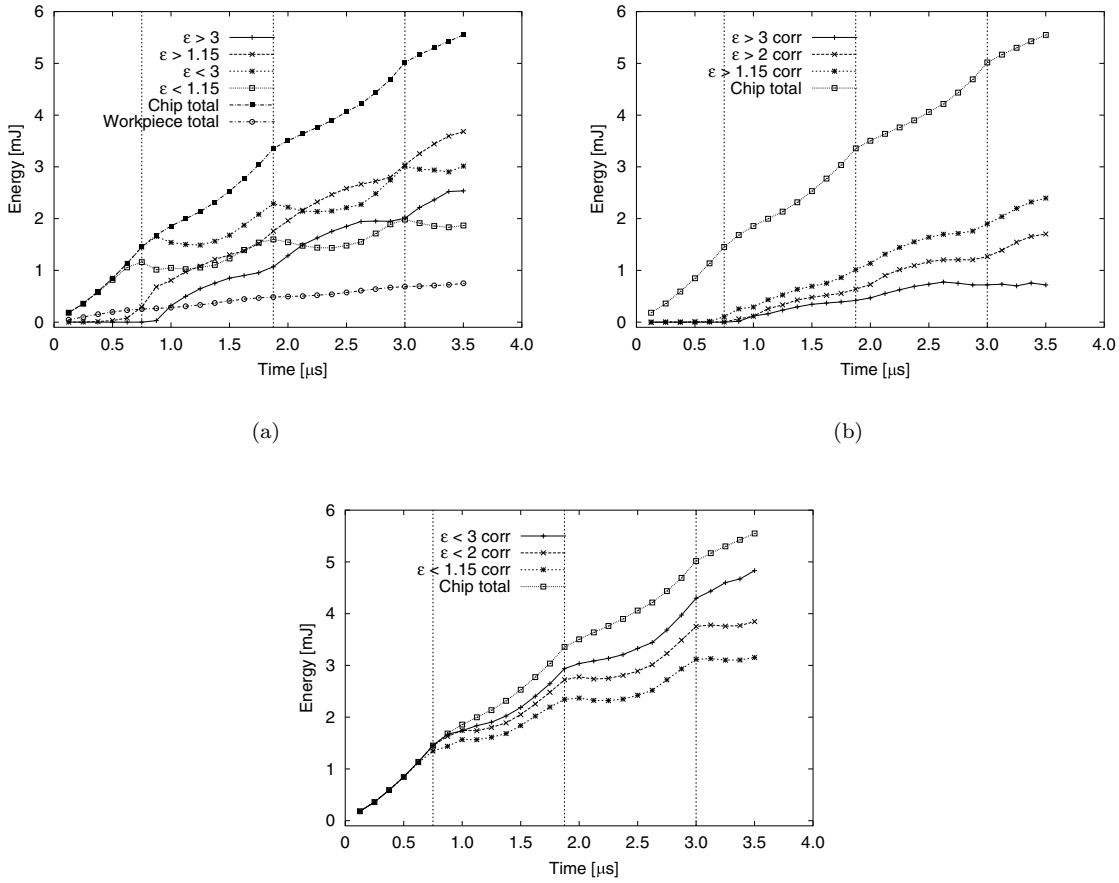

Figure 4: Energy Distribution in Segment and Shear Band for the Simulation Shown in Figure 3.

3.3 Variation of Thermal Conductivity

The shear localization process discussed here is caused by the thermal softening of the material in the shear band, which exceeds the rate-dependent hardening[2]. It should therefore be expected that reducing the thermal conductivity leads to a stronger concentration of heat in the shear zone and therefore also to a stronger segmentation. To study this, the thermal conductivity has been varied by two orders of magnitude in the simulation, as shown in Figure 5. The Figure shows the first shear band in the simulation for reduced, standard, and increased thermal conductivity. As expected, the degree of segmentation decreases as the conductivity is increased.

The cutting force, shown in Figure 6, varies with the conductivity. It is largest for the case of no segmentation. This is not totally obvious, as the deformation of the material in the continuous chip is eased when heat flows into the undeformed material. Comparing the two simulations with the smaller conductivity values, there is no difference in the cutting force during the damming phase of the chip formation process. When shear localization begins, the material with the smaller conductivity deforms more easily, leading to a smaller minimal cutting force. As the degree of segmentation is larger for the smaller conductivity, the cutting force increases at a later time.

[2]As discussed in Section 3.1, Titanium alloys also exhibit isothermal softening, i.e. softening on increasing the strain. This phenomenon causes these alloys to form segmented chips even at very low cutting speeds. However, as this was not accounted for in the material law, equation (1), in these simulations it is only the thermal softening that plays a role.

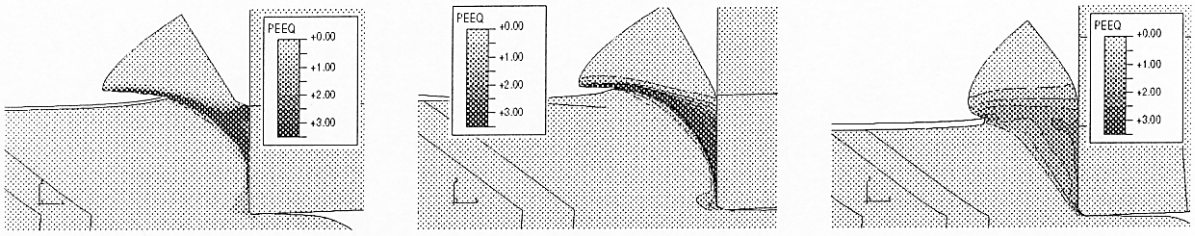

Reduced conductivity | Standard conductivity | Increased conductivity

Figure 5: Equivalent plastic strain for simulations with thermal conductivity varied by a factor of 10. As the strains may become very large inside the shear band, the darkest colour in the scale corresponds to all values larger than 3. The segmentation increases with decreasing thermal coductivity. Model parameters: Cutting depth 35 µm, cutting speed 20 m/s, rake angle 0°.

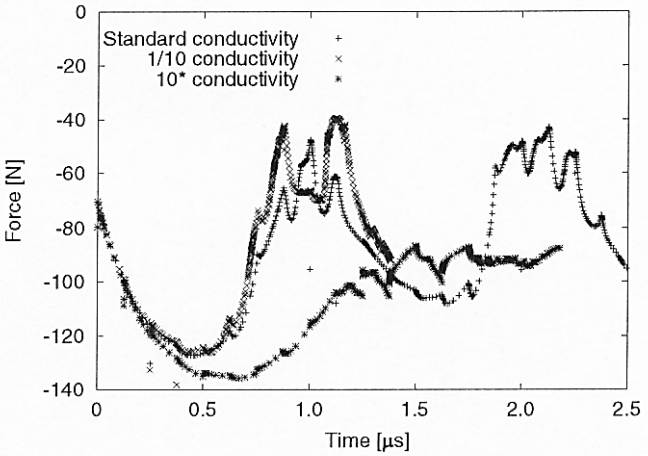

Figure 6: Cutting Force for the Three Simulations Shown in Figure 5.

4 Conclusions

After a brief introduction to the machining process, a finite element model of the chip formation process was presented. The model uses frequent remeshings to avoid mesh distortions and to allow the correct representation of serrated chips with reentrant corners. The choice of a material law describing the plastic behaviour of the material was discussed in some detail, as this poses one of the major problems of any simulation of high-speed cutting. The material law used here should be considered as describing a model material, not as a reliable representation of the behaviour of a certain alloy. Until better material models for adiabatic shearing are available, this approach seems the only feasible way to perform finite element studies of the segmentation process.

A detailed analysis of the deformation process shows that the shear localization begins after the material has been dammed in front of the tool, but different from some models in the literature the shear band is not strongly curved. The energy dissipated in the segment and that in the shear band both contribute significantly to the cutting force. Although the greatest part of the energy is dissipated in the region that forms the shear band, this energy is dissipated in the first phase of the shear localization. A variation of the thermal conductivity shows that chip segmentation may be energetically favorable compared to a segmented chip, but further investigations are necessary to confirm this.

Acknowledgements
Thanks to Arnold Gente and Carsten Siemers for many interesting discussions. Financial support by the Deutsche Forschungsgemeinschaft is gratefully acknowledged.

Literature

1. Bäker, M., Rösler, J., Siemers, C.: Finite Element Simulation of Segmented Chip Formation of Ti6Al4V, Journal Manuf. Sc. & Eng., 124, (2002), 485.
2. Bäker, M., Rösler, J., Siemers, C.: A Finite Element Model of High Speed Metal Cutting with Adiabatic Shearing, Computers & Structures, 80, (2002), 495.
3. El-Magd, E.; Treppmann, C.: Dehnratenabhängige Beschreibung der Fließkurven für erhöhte Temperaturen, Z. Metallkunde, 92, (2001), 888.
4. HKS Inc., USA, *ABAQUS/Standard User's Manual, Version 5.8*, (1998).
5. HKS Inc., USA, *ABAQUS Theory Manual, Version 5.8*, (1998).
6. Hoffmeister, H.-W.; Gente, A.; Weber, T.: Chip Formation at Titanium Alloys under Cutting Speeds of up to 100m/s, Proc. of the 2nd International German and French Conference on High Speed Machining, Darmstadt, (1999).
7. Hou, Z. B.;, Komanduri, R.: Modeling of Thermomechanical Shear Instability in Machining, Int. J. Mech. Sci., 39, (1997), 1273.
8. Huang, J.M.; Black, J.T.: An Evaluation of Chip separation Criteria for the FEM Simulation of Machining, Journal of Manufacturing Science and Engineering, 118, (1996), 545.
9. Marusich, T.D.; Ortiz, M.: Modelling and Simulation of High-Speed Machining, Int. J. Numer. Methods Eng., 38, (1995), 3675.
10. Merchant, M. E.: Mechanics of the Metal Cutting Process. I. Orthogonal Cutting and a Type 2 Chip, J. Appl. Phys., 16, (1945), 267.
11. Nakayama, K.: The Formation of saw Toothed Chips, Proc. Int. Conf. on Prod. Eng., Tokyo, (1974).
12. Ng, E.; Aspinwall, D.: Hard part machining AISI H 13 using AMBORITE AMB 90: a finite element modelling approach, Industrial Diamond Review, 4, (2000), 305.
13. Obikawa T.; Usui, E.: Computational Machining of Titanium Alloy—Finite Element Modeling and a Few Results, J. of Manufacturing Science and Engineering, 118, (1996), 208.
14. Recht, R.F.: A Dynamic Analysis of High Speed Machining, ASME J. of Eng. for Ind., 107, (1985), 309.
15. Sekhon, G.S.; Chenot, J.L.:Numerical simulation of continuous chip formation during non-steady orthogonal cutting, Engineering Computations, 10, (1993), 31.
16. Vyas, A.; Shaw, M.C.: Mechanics of Saw-Tooth Chip Formation in Metal Cutting, J. of Manufacturing Science and Engineering, 121, (1999), 165.

Address: Dr. rer. nat. Martin Bäker, Institut für Werkstoffe, Technische Universität Braunschweig, Langer Kamp 8, D-38106 Braunschweig, Germany, e-mail: martin.baeker@tu-bs.de